

CONSEQUENCE OF STATOR AND ROTOR INUNDATION ON SENSOR LESS ROTOR LOCUS DETECTION MACHINE DESIGN

¹A.RAVEENDRA, ²M.PRINCE, ³K. MALLIKARJUNA

^{1,2&3}Professor, Department of Mechanical Engineering, Malla Reddy Engineering College

(Autonomous), Maisammaguda(H), Gundlapochampally Village, Secunderabad, Telangana State - 500100

Abstract

This paper deals with self-sensing-oriented optimization of synchronous reluctance machines. This kind of machine is among the most challenging to control without the position sensor at low speed. In fact, typical position estimations adopt high-frequency voltage injection which heavily relies on the intrinsic machine saliency. However, both at low and high currents, such saliency is not guaranteed due to the presence of the iron ribs and to the saturation of the iron material, respectively. Furthermore, the estimation algorithm could also become unstable due to the absence of convergence points. The aim of the paper is to tackle this issue, embedding proper sensor less-control cap.

Introduction

Synchronous reluctance machines (SyRM) represent an attractive alternative to induction and PM motors in many applications. One of the advantages is their intrinsic saliency which allows for sensorless position estimation at low speeds using high-frequency (HF) voltage injection [1]–[3]. However, iron cross-saturation reduces the effectiveness of this position estimation algorithm creating an estimation error [4]–[6]. The typical solution for this problem is to add a compensation angle or equivalently tilt the high-frequency voltage vector to correct the estimated position [7], [8]. In case of heavily saturated machine this kind of strategy is not enough, though. In fact, the algorithm could even not converge. This aspect has been analyzed in [9], [10], where different kinds of compensations were proposed to extend the self-

sensing feasibility torque range. Even though these compensation techniques proved to be effective, they require additional effort for the implementation and also some information about the machine magnetic behaviour.

Several papers in the past tried to enhance the self-sensing capability of interior permanent magnet (IPM) motors [5], [11], [12], focusing on avoiding that the Maximum Torque Per Ampere (MTPA) trajectory crosses the point where the current error signal is zero. Despite that, few or no research is available for SyRM, where the convergence issue is different in nature. In this paper, the non-convergence issue is tackled from early electromagnetic design phase, trying to embed the solution into a complete optimization of the motor. The sensorless technique considered hereafter is the injection of high-frequency pulsating voltage along the estimated d-

axis

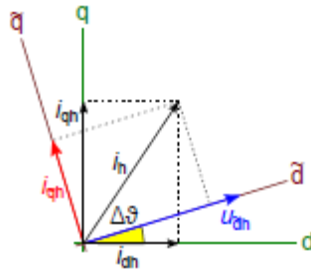


Fig. 1: Estimation error and current error signal.

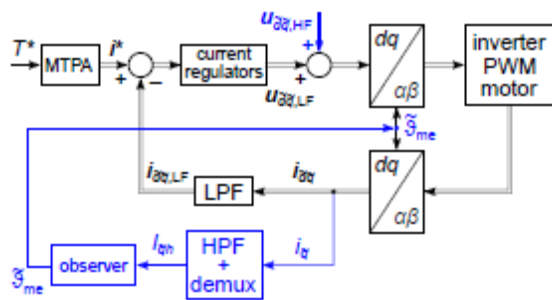


Fig. 2: Control scheme of the electric drive with high-frequency signal injection for rotor position estimation.

Proposed method

This kind of machine is among the most challenging to control without the position sensor at low speed. In fact, typical position estimations adopt high-frequency voltage injection which heavily relies on the intrinsic machine saliency. However, both at low and high currents, such saliency is not guaranteed due to the presence of the iron ribs and to the saturation of the iron material, respectively.

Methodology

Example of a typical optimization

The specifications and the constraints of the machine under analysis are reported in Table I. In particular, the requirement is to obtain about 90 Nm with the highest possible efficiency within the given dimensions. At first, also the stator geometry is a constraint, and its data is also

reported in Table I. A state-of-the-art optimization coupled to finite element analysis (FEA) has been performed in order to assess the feasibility of the design and to get the overall machine performance. The main objectives for synchronous reluctance machines are average torque and torque ripple. Since most of the losses are allocated in the stator and in this optimization the stator is kept the same, the efficiency depends only upon the average torque.

The objectives plane is reported in Fig. 3. Every dot represents a simulated individual. Each evaluation took about

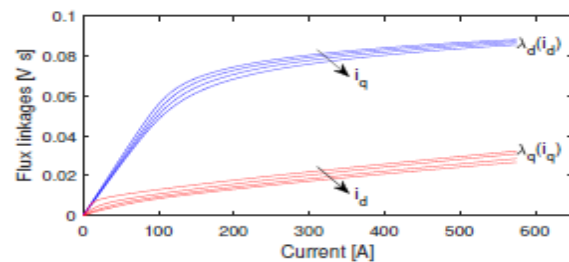


Fig. 4: Flux linkages as functions of the two axes currents.

that for this machine the last achievable torque level without any compensation is at about 45 Nm (49% of the rated one). Since $\lambda_{q\tilde{d}}(\theta)$ stays always negative when convergence problems appear (see Fig. 6), the convergence region can also be found in the whole (i_d, i_q) plane for every working point looking at the maximum value of the $\lambda_{q\tilde{d}}$ waveform: if this value is higher than zero, then there is a zero-crossing and therefore the estimating algorithm converges. Thus, the contour $\lambda_{q\tilde{d}} = 0$ delimits the unfeasible region. In Fig. 8 it can be observed that such a region is quite wide. The cause of this issue is the presence

of harmonics in both ℓ_{-} and ℓ_{dq} along the current circles.

The presence of a second order harmonic is evident (in the figure only a semi-period is shown). The error signal can be computed substituting ℓ_{-} and ℓ_{dq} harmonics into the numerator of (5). Defining ϑ the angle starting from the d-axis, the error angle ϑ is defined through .

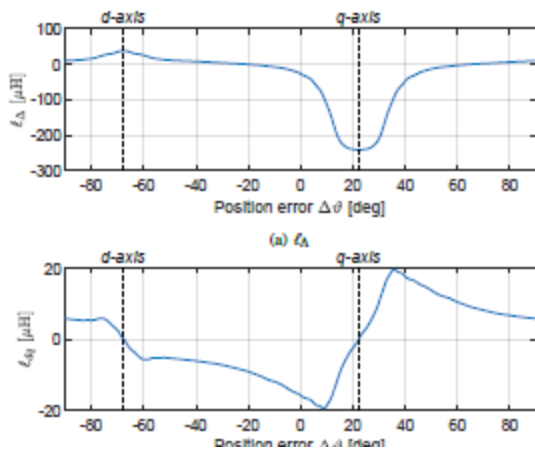


Fig. 9: ℓ_{-} and ℓ_{dq} as functions of position estimation error at rated current

A. First self-sensing-oriented optimization In this optimization there were three objectives: torque ripple, efficiency and cross-saturation differential inductance. The parameters (degrees of freedom) were the three flux barrier angles, the magnetic insulation ratio, the stator split ratio, the stator tooth width and slot height. The results of the first optimization are reported in Fig. 10. It can be observed that the cross-saturation differential inductance ℓ_{-} is proportional to the efficiency. So the higher the efficiency, the higher ℓ_{dq} . Such a quantity strongly depends on the saturation of the machine, which is affected by the geometrical parameters (and so is the torque, thus the efficiency). Larger iron areas improve ℓ_{dq} but negatively affects

the motor torque and so the efficiency. In fact the rotor diameter decreases to leave more space for the stator yoke, and the slots shrink to obtain larger teeth. As a consequence the slot area has to decrease, and so the copper losses increase.

In this optimization the Pareto front is a 3D surface. In Fig. 10 the efficiency and ℓ_{dq} are reported in the two axes, while the torque ripple is displayed through the size of the markers: the bigger the marker, the lower the ripple. The average torque is not an objective now, but it is implicitly taken into account in the torque ripple and in the efficiency. Some individuals on the Pareto front were selected for the complete

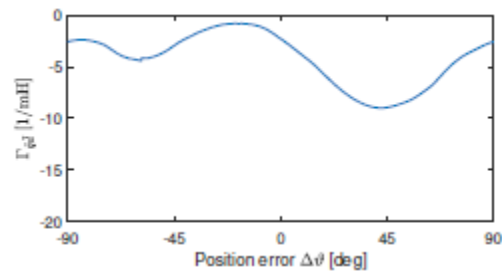


Fig. 16: Γ_{qd} as a function of ϑ for the base point.

course, this improvement comes at a cost: the efficiency drops to about 91.4 %. The torque ripple has been minimized through a second optimization to a value of about 5 %. The extension of the self-sensing range is evident also looking at Fig. 15 and comparing it to Fig. 8. The unfeasible region now is greatly reduced and it presents lower absolute values.

In Fig. 14 the geometry analyzed is shown and compared to the one first studied. The differences are evident. In particular the rotor diameter is smaller, but that does not affect the torque capability of the machine. Overall, there is now more iron in the stator, both in the yoke and in the teeth. As

a result, the slot area becomes smaller, which explains the decrease in the efficiency.

Finally, Fig. 16 reports the waveform of \hat{q}^d as a function of the estimation error for the base point. Comparing it with Fig. 6, it can be noted that the behavior is improved even though it still does not cross the x-axis. In fact, it has less negative offset, and also the peak before $\theta = 0^\circ$ is more pronounced and closer to zero. This means that smaller current and angle compensations are needed.

Conclusion

In this paper a HF-injection self-sensing-oriented optimization scheme has been presented. A heavily saturated synchronous reluctance motor has been selected as a case study. At first, a typical optimization has been performed on the rotor of the machine. The torque range for sensorless control was rather limited. After that, the source of the issue has been highlighted, together with the possible mitigating solutions. These solutions were embedded into the optimization algorithm, in two different ways. Even though the solution found was notable to exhibit self-sensing capability at the maximum torque, the torque range has been greatly extended to about 87% of the rated torque. It has been demonstrated that the factor that affects the convergence of the observer the most is R_s , which is mainly due to the stator saturation. However, the rotor should be designed accordingly to guarantee a high average torque, high efficiency and low torque ripple. Finally, it has been deduced that a better self-sensing capability comes at the cost of lower efficiency. This fact highlights the

importance of considering HF-injection sensorless control at early design phases.

References

- [1] M. Corley and R. Lorenz, "Rotor position and velocity estimation for a permanent magnet synchronous machine at standstill and high speeds," *IEEE Transactions on Industry Applications*, vol. 34, no. 4, pp. 784–789, 1998.
- [2] Y. Jeong, R. D. Lorenz, T. M. Jahns, and S. Sul, "Initial Rotor Position Estimation of an Interior Permanent Magnet Synchronous Machine using Carrier-Frequency Injection Methods," *IEEE Transactions on Industry Applications*, vol. 41, no. 1, pp. 1218–1223, 2005.
- [3] S. C. Yang and Y. L. Hsu, "Full Speed Region Sensorless Drive of Permanent-Magnet Machine Combining Saliency-Based and Back-EMF Based Drive," *IEEE Transactions on Industrial Electronics*, vol. 64, no. 2, pp. 1092–1101, 2017.
- [4] P. Guglielmi, M. Pastorelli, and A. Vagati, "Cross-saturation effects in IPM motors and related impact on sensorless control," *IEEE Transactions on Industry Applications*, vol. 42, no. 6, pp. 1516–1522, 2006.
- [5] N. Bianchi, E. Fornasiero, and S. Bolognani, "Effect of stator and rotor saturation on sensorless rotor position detection," *IEEE Transactions on Industry Applications*, vol. 49, no. 3, pp. 1333–1342, 2013.
- [6] M. Barcaro, M. Morandini, T. Pradella, N. Bianchi, and I. Furlan, "Iron saturation impact on high frequency sensorless control of synchronous permanent magnet motor," *Proceedings - 2016 22nd International Conference on Electrical Machines, ICEM 2016*, vol. 53, no. 6, pp.

1085–1091, 2016.

[7] Satyanarayana, P. and Subramanyam Pavuluri, D.A., 2013. PARAMETRIC MODELING AND DYNAMIC CHARACTERIZATION FOR STATIC STRENGTH OF STEAM TURBINE MOVING BLADES. *International Journal of Innovative Research in Science, Engineering and Technology*, 2(7).

[8] PAVULURI, S. and KUMAR, D.A.S., 2013. „“ Experimental Investigation On Design Of High Pressure Steam Turbine Blade””. *International Journal of Innovative Research in Science, Engineering and Technology*, 2(5), pp.1469-1476.

[9] Sreenivas, P., Kumar, A.S. and Subramanyam Pavuluri, D.A., 2013.

Investigations on transient dynamic response of functionally graded materials. a a, 1, p.2.

[10] Pavuluri, S., Rajashekar, B. and Damodhar, B., Process of Press Tool Design and its Manufacturing for Blanking Operation.

[11] KUMAR, S.S. and SUBRAMANYAM, P., DESIGN AND WEIGHT OPTIMIZATION OF OIL PAN BY FE ANALYSIS.

[12] PAVULURI, S. and KUMAR, D.A.S., 2013. „“ Experimental Investigation On Design Of High Pressure Steam Turbine Blade””. *International Journal of Innovative Research in Science, Engineering and Technology*, 2(5), pp.1469-1476.